

---

# An intriguing failing of convolutional neural networks and the CoordConv solution

---

**Rosanne Liu<sup>1</sup>**

[rosanne@uber.com](mailto:rosanne@uber.com)

**Joel Lehman<sup>1</sup>**

[joel.lehman@uber.com](mailto:joel.lehman@uber.com)

**Piero Molino<sup>1</sup>**

[piero@uber.com](mailto:piero@uber.com)

**Felipe Petroski Such<sup>1</sup>**

[felipe.such@uber.com](mailto:felipe.such@uber.com)

**Eric Frank<sup>1</sup>**

[mysterefrank@uber.com](mailto:mysterefrank@uber.com)

**Alex Sergeev<sup>2</sup>**

[asergeev@uber.com](mailto:asergeev@uber.com)

**Jason Yosinski<sup>1</sup>**

[yosinski@uber.com](mailto:yosinski@uber.com)

## Abstract

Few ideas have enjoyed as large an impact on deep learning as convolution. For any problem involving pixels or spatial representations, common intuition holds that convolutional neural networks may be appropriate. In this paper we show a striking counterexample to this intuition via the seemingly trivial *coordinate transform problem*, which simply requires learning a mapping between coordinates in  $(x, y)$  Cartesian space and coordinates in one-hot pixel space. Although convolutional networks would seem appropriate for this task, we show that they fail spectacularly. We demonstrate and carefully analyze the failure first on a toy problem, at which point a simple fix becomes obvious. We call this solution CoordConv, which works by giving convolution access to its own input coordinates through the use of extra coordinate channels. Without sacrificing the computational and parametric efficiency of ordinary convolution, CoordConv allows networks to learn either perfect translation invariance or varying degrees of translation dependence, as required by the end task. CoordConv solves the coordinate transform problem with perfect generalization and 150 times faster with 10–100 times fewer parameters than convolution. This stark contrast raises the question: to what extent has this inability of convolution persisted insidiously inside other tasks, subtly hampering performance from within? A complete answer to this question will require further investigation, but we show preliminary evidence that swapping convolution for CoordConv can improve models on a diverse set of tasks. Using CoordConv in a GAN produced less mode collapse as the transform between high-level spatial latents and pixels becomes easier to learn. A Faster R-CNN detection model trained on MNIST detection showed 24% better IOU when using CoordConv, and in the Reinforcement Learning (RL) domain agents playing Atari games benefit significantly from the use of CoordConv layers.

## 1 Introduction

Convolutional neural networks (CNNs) [16] have enjoyed immense success as a key tool for enabling effective deep learning in a broad array of applications, like modeling natural images [31, 15], images of human faces [14], audio [28], and enabling agents to play games in domains with synthetic imagery like Atari [18].

Although straightforward CNNs excel at many tasks, in many other cases progress has been accelerated through the development of specialized layers that complement the abilities of CNNs. Detection

---

<sup>1</sup>Uber AI Labs, San Francisco, CA, USA

<sup>2</sup>Uber Technologies, Seattle, WA, USA

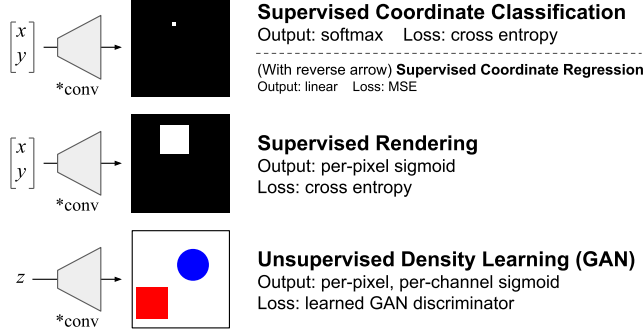


Figure 1: Toy tasks considered in this paper. The  $*\text{conv}$  block represents a network comprised of one or more convolution, deconvolution (convolution transpose), or CoordConv layers. Experiments compare networks with no CoordConv layers to those with one or more.

models like Faster R-CNN [23] make use of layers to compute coordinate transforms and focus attention, spatial transformer networks [12] make use of differentiable cameras to transform data from the output of one CNN into a form more amenable to processing with another, and some generative models like DRAW [6] iteratively perceive, focus, and refine a canvas rather than using a single pass through a CNN to generate an image. These models were all created by neural network designers that intuited some inability or misguided inductive bias of standard CNNs and then devised a workaround.

In this work, we expose and analyze a generic inability of CNNs to transform spatial representations between two different types: from a dense Cartesian representation to a sparse, pixel-based representation or in the opposite direction. Though such transformations would seem simple for networks to learn, it turns out to be more difficult than expected, at least when models are comprised of the commonly used stacks of convolutional layers. While straightforward stacks of convolutional layers excel at tasks like image classification, they are not quite the right model for coordinate transform.

The main contributions of this paper are as follows:

1. We define a simple toy dataset, *Not-so-Clevr*, which consists of squares randomly positioned on a canvas (Section 2).
2. We define the *CoordConv* operation, which allows convolutional filters to know where they are in Cartesian space by adding extra, hard-coded input channels that contain coordinates of the data seen by the convolutional filter. The operation may be implemented via a couple extra lines of Tensorflow (Section 3).
3. Throughout the rest of the paper, we examine the coordinate transform problem starting with the simplest scenario and ending with the most complex. Although results on toy problems should generally be taken with a degree of skepticism, starting small allows us to pinpoint the issue, exploring and understanding it in detail. Later sections then show that the phenomenon observed in the toy domain indeed appears in more real-world settings.

We begin by showing that coordinate transforms are surprisingly difficult even when the problem is *small and supervised*. In the *Supervised Coordinate Classification* task, given a pixel’s  $(x, y)$  coordinates as input, we train a CNN to highlight it as output. The *Supervised Coordinate Regression* task entails the inverse: given an input image containing a single white pixel, output its coordinates. We show that both problems are harder than expected using convolutional layers but become trivial by using a CoordConv layer (Section 4).

4. The *Supervised Rendering* task adds complexity to the above by requiring a network to paint a full image from the Not-so-Clevr dataset given the  $(x, y)$  coordinates of a square in the image. The task is still fully supervised, but as before, the task is difficult to learn for convolution and trivial for CoordConv (Section 4.3).
5. We show that replacing convolutional layers with CoordConv improves performance in a variety of tasks. On two-object Sort-of-Clevr [25] images, Generative Adversarial Networks (GANs) and Variational Autoencoders (VAEs) using CoordConv exhibit less mode collapse, perhaps because ease of learning coordinate transforms translates to ease of using latents to span a 2D Cartesian space. Larger GANs on bedroom scenes with CoordConv offer

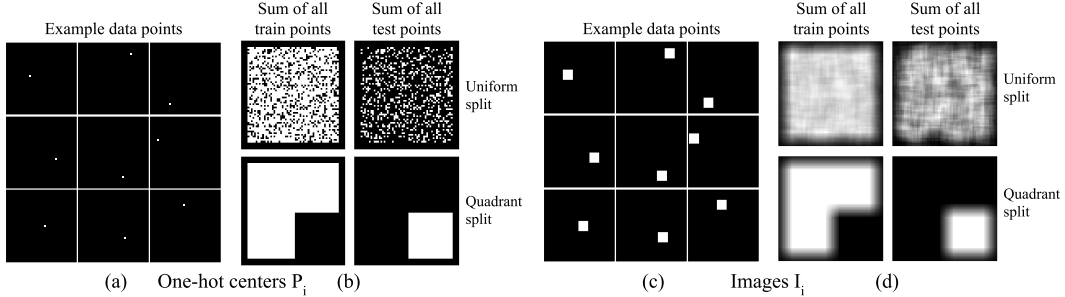


Figure 2: The Not-so-Clevr dataset. **(a)** Example one-hot center images  $P_i$  from the dataset. **(b)** The pixelwise sum of the entire train and test splits for uniform vs. quadrant splits. **(c)** and **(d)** Analogous depictions of the canvas images  $I_i$  from the dataset. Best viewed electronically with zoom.

geometric translation that was never observed in regular GAN. Adding CoordConv to a Faster R-CNN produces much better object boxes and scores. Finally, agents learning to play Atari games obtain significantly higher scores on some but not all games, and they never do significantly worse (Section 5).

With reference to the above numbered contributions, the reader may be interested to know that the course of this research originally progressed in the  $5 \rightarrow 2$  direction as we debugged why progressively simpler problems continued to elude straightforward modeling. But for ease of presentation, we give results in the  $2 \rightarrow 5$  direction. A progression of the toy problems considered is shown in Figure 1.

## 2 Not-so-Clevr dataset

We define the Not-so-Clevr dataset and make use of it for the first experiments in this paper. The dataset is a single-object, grayscale version of Sort-of-CLEVR [25], which itself is a simpler version of the Clevr dataset of rendered 3D shapes [13]. Not-so-Clevr consists of  $9 \times 9$  squares placed on a  $64 \times 64$  canvas. Square positions are restricted such that the entire square lies within the  $64 \times 64$  grid, so that square centers fall within a slightly smaller possible area of  $56 \times 56$ . Enumerating these possible center positions results in a dataset with a total of 3,136 examples. For each example square  $i$ , the dataset contains three fields:

- $C_i \in \mathbb{R}^2$ , its center location in  $(x, y)$  Cartesian coordinates,
- $P_i \in \mathbb{R}^{64 \times 64}$ , a one-hot representation of its center pixel, and
- $I_i \in \mathbb{R}^{64 \times 64}$ , the resulting  $64 \times 64$  image of the square painted on the canvas.

We define two train/test splits of these 3,136 examples: *uniform*, where all possible center locations are randomly split 80/20 into train vs. test sets, and *quadrant*, where three of four quadrants are in the train set and the fourth quadrant in the test set. Examples from the dataset and both splits are depicted in Figure 2. To emphasize the simplicity of the data, we note that this dataset may be generated in only a line or two of Python using a single convolutional layer with filter size  $9 \times 9$  to paint the squares from a one-hot representation.<sup>3</sup>

## 3 The CoordConv layer

The proposed CoordConv layer is a simple extension to the standard convolutional layer. We assume for the rest of the paper the case of two spatial dimensions, though operators in other dimensions follow trivially. Convolutional layers are used in a myriad of applications because they often work well, perhaps due to some combination of three factors: they have relatively few learned parameters, they are fast to compute on modern GPUs, and they learn a function that is translation invariant (a translated input produces a translated output).

<sup>3</sup>For example, ignoring import lines and train/test splits:

```
onehots = np.pad(np.eye(3136).reshape((3136, 56, 56, 1)), ((0,0), (4,4), (4,4), (0,0)), "constant");
images = tf.nn.conv2d(onehots, np.ones((9, 9, 1, 1)), [1]*4, "SAME")
```

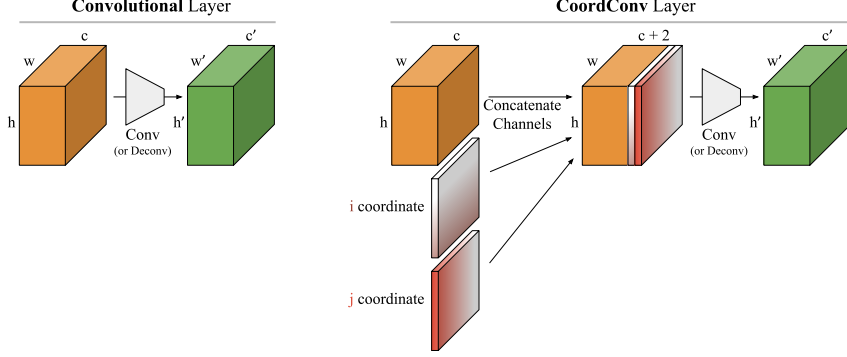


Figure 3: Comparison of 2D convolutional and CoordConv layers. **(left)** A standard convolutional layer maps from a representation block with shape  $h \times w \times c$  to a new representation of shape  $h' \times w' \times c'$ . **(right)** A CoordConv layer has the same functional signature, but accomplishes the mapping by first concatenating extra channels to the incoming representation. These channels contain hard-coded coordinates, the most basic version of which is one channel for the  $i$  coordinate and one for the  $j$  coordinate, as shown above. Other derived coordinates may be input as well, like the radius coordinate used in ImageNet experiments (Section 5).

The CoordConv layer keeps the first two of these properties—few parameters and efficient computation—but allows the network to learn to keep or to discard the third—translation invariance—as is needed for the task being learned. It may appear that doing away with translation invariance will hamper networks’ abilities to learn generalizable functions. However, as we will see in later sections, allocating a small amount of network capacity to model non-translation invariant aspects of a problem can enable far more trainable models that also generalize far better.

The CoordConv layer can be implemented as a simple extension of standard convolution in which extra channels are instantiated and filled with (constant, untrained) coordinate information, after which they are concatenated channel-wise to the input representation and a standard convolutional layer is applied. Figure 3 depicts the operation where two coordinates,  $i$  and  $j$ , are added. Concretely, the  $i$  coordinate channel is an  $h \times w$  rank-1 matrix with its first row filled with 0’s, its second row with 1’s, its third with 2’s, etc. The  $j$  coordinate channel is similar, but with columns filled in with constant values instead of rows. In all experiments, we apply a final linear scaling of both  $i$  and  $j$  coordinate values to make them fall in the range  $[-1, 1]$ . For convolution over two dimensions, two  $(i, j)$  coordinates are sufficient to completely specify an input pixel, but if desired, further channels can be added as well to bias models toward learning particular solutions. In some of the experiments that follow, we have also used a third channel for an  $r$  coordinate, where  $r = \sqrt{(i - h/2)^2 + (j - w/2)^2}$ . The full implementation of the CoordConv layer is provided in Section S8. Let’s consider next a few properties of this operation.

**Number of parameters.** Ignoring bias parameters (which are not changed), a standard convolutional layer with square kernel size  $k$  and with  $c$  input channels and  $c'$  output channels will contain  $cc'k^2$  weights, whereas the corresponding CoordConv layer will contain  $(c + d)c'k^2$  weights, where  $d$  is the number of coordinate dimensions used (e.g. 2 or 3). The relative increase in parameters is small to moderate, depending on the original number of input channels.<sup>4</sup>

**Translation invariance and relations to other work.** CoordConv is similar to a few other approaches, so we draw comparisons from several directions. CoordConv with weights connected to input coordinates set by initialization or learning to zero will be translation invariant and thus mathematically equivalent to ordinary convolution. If weights are nonzero, the function will contain some degree of translation dependence, the precise form of which will ideally depend on the task

<sup>4</sup>A CoordConv layer implemented via the channel concatenation discussed entails an increase of  $dc'k^2$  weights. However, if  $k > 1$ , not all  $k^2$  connections from coordinates to each output unit are necessary, as spatially neighboring coordinates do not provide new information. Thus, if one cares acutely about minimizing the number of parameters and operations, a  $k \times k$  conv may be applied to the input data and a  $1 \times 1$  conv to the coordinates, then the results added. In this paper we have used the simpler, if marginally inefficient, channel concatenation version that applies a single convolution to both input data and coordinates. However, almost all experiments use  $1 \times 1$  filters with CoordConv.

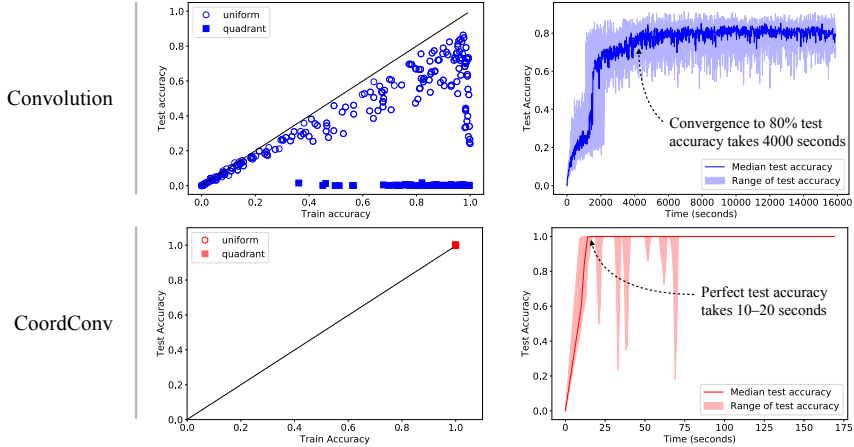


Figure 4: Performance of convolution and CoordConv on Supervised Coordinate Classification. **(left column)** Final test vs. train accuracy. On the easier uniform split, convolution never attains perfect test accuracy, though the largest models memorize the training set. On the quadrant split, generalization is almost zero. CoordConv attains perfect train and test accuracy on both splits. One of the main results of this paper is that the translation invariance in ordinary convolution does not lead to coordinate transform generalization even to neighboring pixels! **(right column)** Test accuracy vs. training time of the best uniform-split models from the left plot (any reaching final test accuracy  $\geq 0.8$ ). The convolution models never achieve more than about 86% accuracy, and training is slow: the fastest learning models still take over an hour to converge. CoordConv models learn several hundred times faster, attaining perfect accuracy in seconds.

being solved. Similar to locally connected layers with unshared weights, CoordConv allows learned translation dependence, but by contrast it requires far fewer parameters:  $(c + d)c'k^2$  vs.  $hwcc'k^2$  for spatial input size  $h \times w$ . Note that all CoordConv weights, even those to coordinates, are shared across all positions, so translation dependence comes only from the specification of coordinates; one consequence is that, as with ordinary convolution but unlike locally connected layers, the operation can be expanded outside the original spatial domain if the appropriate coordinates are extrapolated.

CoordConv layers are also related to Compositional Pattern Producing Networks (CPPNs) [27]. CPPNs implement functions from coordinates in arbitrarily many dimensions to one or more output values. For example, with two input dimensions and  $N$  output values, this can be thought of as painting  $N$  separate grayscale pictures. CoordConv can then be thought of as a conditional CPPN where output values depend not only on coordinates but also on incoming data. In one CPPN-derived work [10], researchers did train networks that take as input both coordinates and incoming data for their use case of synthesizing a drum track that could derive both from a time coordinate and from other instruments (input data) and trained using interactive evolution. With respect to that work, we may see CoordConv as a simpler, single-layer mechanism that fits well within the paradigm of training large networks with gradient descent on GPUs. In a similar vein, research on convolutional sequence to sequence learning [5] has used fixed and learned position embeddings at the input layer; in that work, positions were represented via an overcomplete basis that is added to the incoming data rather than being compactly represented and input as separate channels. In some cases using overcomplete sine and cosine bases has seemed to work well [29].

Connections can also be made to mechanisms of spatial attention [12] and to generative models that separately learn what and where to draw [7, 22]. While such works might appear to provide alternative solutions to the problem explored in this paper, in reality, similar coordinate transforms are often embedded within such models (e.g. a spatial transformer network contains a localization network that regresses from an image to a coordinate-based representation [12]) and might also benefit from CoordConv layers. Finally, challenges in learning coordinate transformations are not unknown in machine learning, as learning a Cartesian-to-polar coordinate transform forms the basis of the classic two-spirals classification problem [3].

## 4 Supervised Coordinate tasks

### 4.1 Supervised Coordinate Classification

The first and simplest task we consider is Supervised Coordinate Classification. Illustrated at the top of Figure 1, given an  $(x, y)$  coordinate as input, a network must learn to paint the correct output pixel. This is simply a multi-class classification problem where each pixel is a class. Why should we study such a toy problem? If we expect to train generative models that can transform high level latents like horizontal and vertical position into pixel data, solving this toy task would seem a simple prerequisite. We later verify that performance on this task does in fact predict performance on larger problems.

In Figure 4 we depict training vs. test accuracy on the task for both uniform and quadrant train/test splits. For convolutional models<sup>5</sup> on uniform splits, we find models that generalize somewhat, but 100% test accuracy is never achieved, with the best model achieving only 86% test accuracy. This is surprising: because of the way the uniform train/test splits were created, all test pixels are close to multiple train pixels. Thus, we reach a first striking conclusion: *learning a smooth function from  $(x, y)$  to one-hot pixel is difficult for convolutional networks, even when trained with supervision, and even when supervision is provided on all sides*. Further, training a convolutional model to 86% accuracy takes over an hour and requires about 200k parameters (see Section S1 in the Supplementary Information for details on model architectures, and Section S2 for details on training). On the quadrant split, convolutional models are unable to generalize at all. Figure 5 shows sums over training set and test set predictions, showing visually both the memorization of the convolutional model and its lack of generalization.

In striking contrast, CoordConv models attain perfect performance on both data splits and do so with only 7.5k parameters and in only 10–20 seconds. The parsimony of parameters further confirms they are simply more appropriate models for the task of coordinate transform [24, 9, 17].

### 4.2 Supervised Coordinate Regression

Because of the surprising difficulty of learning to transform Cartesian coordinates into a pixel-based representation, we also examine whether the inverse transformation (i.e. from pixel-based to Cartesian coordinates) is equally difficult. Note that this sort of transform is the type that could be employed by a VAE encoder or GAN discriminator to transform pixel information into higher level latents encoding locations of objects in a scene. While a standard convolutional network can fit the uniform training split given 85k parameters and generalizes well (less than half a pixel error on average), that same architecture completely fails on the quadrant split. A smaller fully-convolutional architecture (12k parameters) can be tuned to achieve limited generalization on the quadrant split (around five pixels error on average), as shown in Figure 5, but performs poorly on the uniform split. In contrast, a 900 parameter CoordConv model, where a single CoordConv layer is followed by several layers of standard convolution, trains quickly and generalizes in both the uniform and quadrant splits. See Section S3 in Supplementary Information for more details. These results suggest that the inverse transformation requires similar considerations to solve as the Cartesian-to-pixel transformation.

### 4.3 Supervised Rendering

Moving beyond the domain of single pixel coordinate transforms, we compare performance of convolutional vs. CoordConv networks on the Supervised Rendering task, which requires a network to produce a  $64 \times 64$  image with a square painted centered at the given  $(x, y)$  location. As shown in Figure 6, we observe the same stark contrast between convolution and CoordConv. Architectures used for both models can be seen in Section S1 in the Supplementary Information, along with further plots, details of training, and hyperparameter sweeps given in Section S4.

## 5 Applicability to Image Classification, Object Detection, Generative Modeling, and Reinforcement Learning

Given the starkly contrasting results above, it is natural to ask how much the demonstrated inability of convolution at coordinate transforms infects other tasks. Does the coordinate transform hurdle persist insidiously inside other tasks, subtly hampering performance from within? Or do networks skirt the issue by learning around it, perhaps by representing space differently, e.g. via non-Cartesian

---

<sup>5</sup>For classification, convolutions and CoordConvs are actually deconvolutional on certain layers when resolutions must be expanded, but we refer to the models as conv or CoordConv for simplicity.

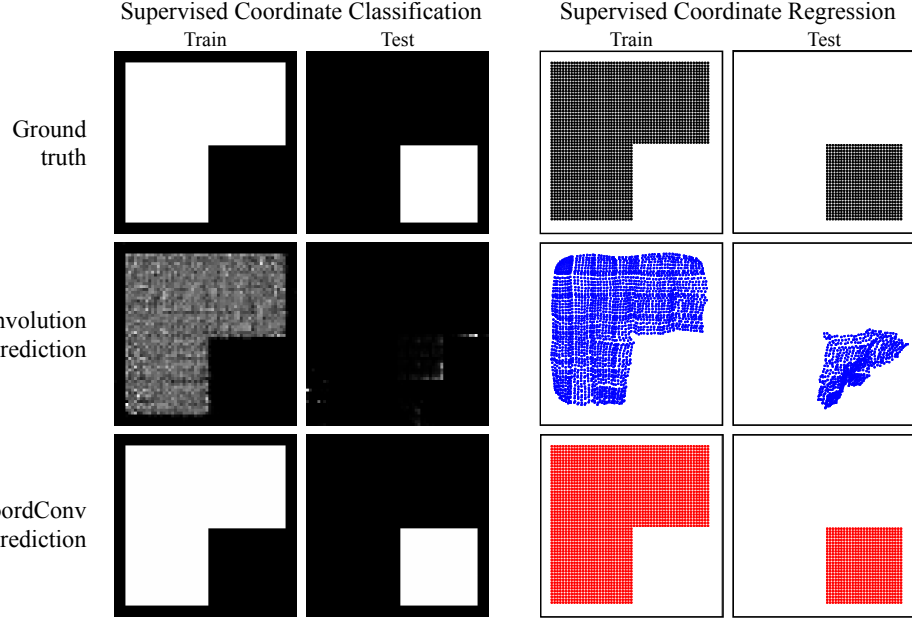


Figure 5: Comparison of convolutional and CoordConv models on the Supervised Coordinate Classification and Regression tasks, on a quadrant split. (**left column**) Results on the seemingly simple classification task where the network must highlight one pixel given its  $(x, y)$  coordinates as input. Images depict ground truth or predicted probabilities summed across the entire train or test set and then normalized to make use of the entire black to white image range. Thus, e.g., the top-left image shows the sum of all train set examples. The conv predictions on the train set cover it well, although the amount of noise in predictions hints at the difficulty with which this model eventually attained 99.6% train accuracy by memorization. The conv predictions on the test set are almost entirely incorrect, with two pixel locations capturing the bulk of the probability for all locations in the test set. By contrast, the CoordConv model attains 100% accuracy on both the train and test sets. (**right column**) The regression task poses the inverse problem: predict real-valued  $(x, y)$  coordinates from a one-hot pixel input. As before, the conv model memorizes poorly and largely fails to generalize, while the CoordConv model fits train and test set perfectly. Thus we observe the coordinate transform problem to be difficult in both directions.

representations like grid cells [1, 4, 2]? A complete answer to this question is beyond the scope of this paper, but encouraging preliminary evidence shows that swapping Conv for CoordConv can improve a diverse set of models — including ResNet-50, Faster R-CNN, GANs, VAEs, and RL models.

**ImageNet Classification** Adding a single extra  $1 \times 1$  CoordConv layer with 8 output channels improves ResNet-50 [8] Top-5 accuracy on average by 0.04%. The result is obtained from five runs of each model, using distributed training on 100 GPUs by using Horovod [26]. See Section S5 in Supplementary Information for details.

**Object Detection** In object detection, models look at pixel space and output bounding boxes in Cartesian space. This creates a natural coordinate transform problem which makes CoordConv seemingly a natural fit. On a simple problem of detecting MNIST digits scattered on a canvas, we found the test intersection-over-union (IOU) of a Faster R-CNN network improved by 24% when using CoordConv. See Section S6 in Supplementary Information for details.

**Generative Modeling** Well-trained generative models can generate visually compelling images [20, 14, 31], but careful inspection can reveal mode collapse: images are of an attractive quality, but sample diversity is far less than diversity present in the dataset. Mode collapse can occur in many dimensions, including those having to do with content, style, or position of components of a scene. We hypothesize that mode collapse of position may be due to the difficulty of learning straightforward transforms from a high-level latent space containing coordinate information to pixel space and that using CoordConv could help. First we investigate a simple task of generating colored shapes with,

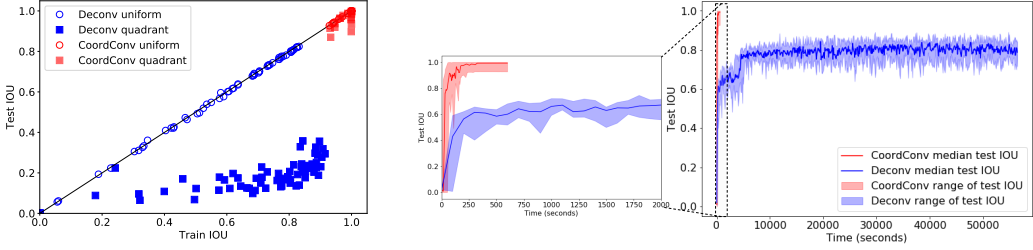


Figure 6: Results on the Supervised Rendering task. As with the Supervised Coordinate Classification and Regression tasks, we see the same vast separation in training time and generalization between convolution models and CoordConv models. (**left**) Test intersection over union (IOU) vs Train IOU. We show all attempted models on the uniform and quadrant splits, including some CoordConv models whose hyperparameter selections led to worse than perfect performance. (**right**) Test IOU vs. training time of the best uniform-split models from the left plot (any reaching final test IOU  $\geq 0.8$ ). Convolution models never achieve more than about IOU 0.83, and training is slow: the fastest learning models still take over two hours to converge vs. about a minute for CoordConv models.

in particular, all possible geometric locations, using both GANs and VAEs. Then we scale up the problem to Large-scale Scene Understanding (LSUN) [30] bedroom scenes with DCGAN [21], through distributed training using Horovod [26].

Using GANs to generate simple colored objects, Figure 7a-d show sampled images and model collapse analyses. We observe that a convolutional GAN exhibits collapse of a two-dimensional distribution to a one-dimensional manifold. The corresponding CoordConv GAN model generates objects that better cover the 2D Cartesian space while using 7% of the parameters of the conv GAN. Details of the dataset and training can be seen in Section S7.1 in the Supplementary Information. A similar story with VAEs is discussed in Section S7.2.

With LSUN, samples are shown in Figure 7e, and more in Section S7.3 in the Supplementary Information. We observe (1) qualitatively comparable samples when drawing randomly from each model, and (2) geometric translating behavior during latent space interpolation.

Latent space interpolation<sup>6</sup> demonstrates that in generating colored objects, motions through latent space generate coordinated object motion. In LSUN, while with convolution we see frozen objects fading in and out, with CoordConv, we instead see smooth geometric transformations including translation and deformation.

**Reinforcement Learning** Adding a CoordConv layer to an actor network within A2C [19] produces significant improvements on some games, but not all. Results are shown in Figure 8. We used OpenAI baselines<sup>7</sup> implementation and default parameters on these experiments. We also tried adding CoordConv to our own implementation of Distributed Prioritized Experience Replay (Ape-X) [11], but we did not notice any immediate difference.

## 6 Conclusion and Future Work

We have shown the curious inability of CNNs to model the coordinate transform task, shown a simple fix in the form of the CoordConv layer, and given results that suggest including these layers can boost performance in a wide range of applications. Future work will further evaluate the benefits of CoordConv in large-scale datasets, exploring its impact in detection, language tasks, video prediction, with spatial transformer networks [12], and with cutting-edge generative models [6].

## Acknowledgments

The authors gratefully acknowledge Zoubin Ghahramani, Peter Dayan, and Ken Stanley for insightful discussions. We are also grateful to Paul Mikesell, Leon Rosenshein, and the entire OpusStack Team inside Uber for providing our computing platform and for technical support.

<sup>6</sup><http://r.yosinski.com/coordconv-interp>

<sup>7</sup><https://github.com/openai/baselines/>

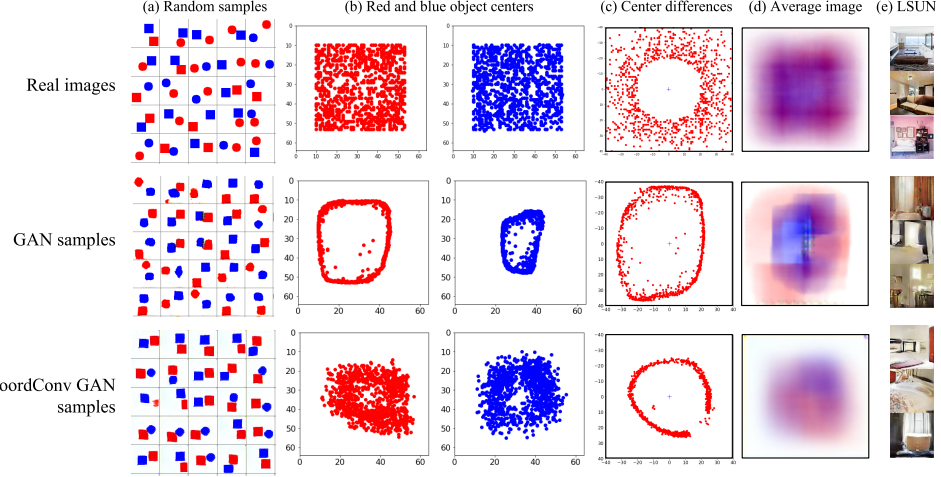


Figure 7: Real images and generated images by GAN and CoordConv GAN. Both models, when trained well, learn the basic concepts: two objects per image, one red and one blue, their size is fixed, and their positions can be random (**column 1**). However, plotting the spread of object centers over 1000 samples, we see that CoordConv GAN samples cover the space better, while GAN samples exhibit mode collapse on where objects can be (**column 2 and 3**). In terms of relative locations between the two objects, both model exhibit a certain level of model collapse (**column 4**). The averaged image of CoordConv GAN is also smoother and closer to real (**column 5**). With LSUN, sampled images are shown (**column 6**). All models used in generation are the best out of many runs.

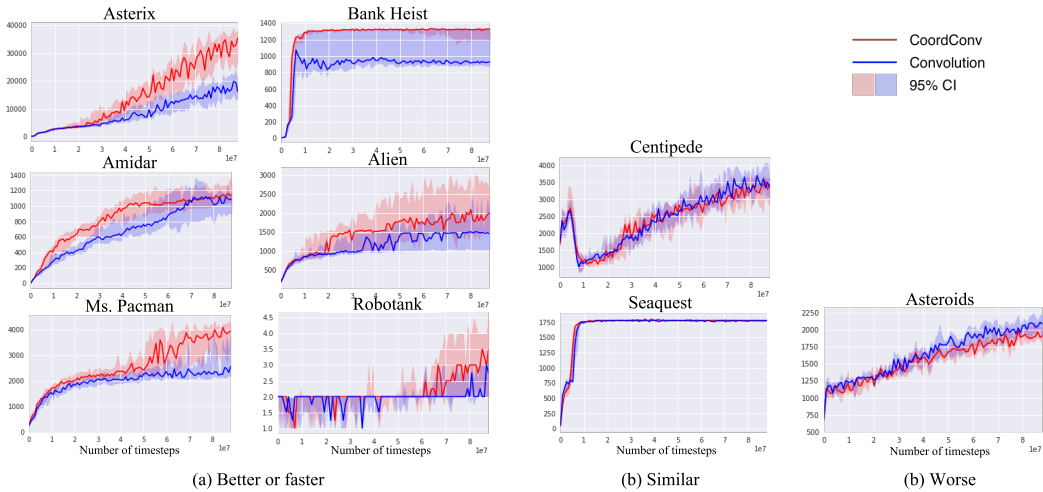


Figure 8: Results using A2C to train on Atari games. Out of 9 games, (a) in 6 CoordConv improves over convolution, (b) in 2 performs similarly, and (c) on 1 it is slightly worse.

## References

- [1] Andrea Banino, Caswell Barry, Benigno Uria, Charles Blundell, Timothy Lillicrap, Piotr Mirowski, Alexander Pritzel, Martin J Chadwick, Thomas Degrif, Joseph Modayil, et al. Vector-based navigation using grid-like representations in artificial agents. *Nature*, page 1, 2018.
- [2] C. J. Cueva and X.-X. Wei. Emergence of grid-like representations by training recurrent neural networks to perform spatial localization. *ArXiv e-prints*, March 2018.
- [3] Scott E Fahlman and Christian Lebiere. The cascade-correlation learning architecture. In *Advances in neural information processing systems*, pages 524–532, 1990.
- [4] Mathias Franzius, Henning Sprekeler, and Laurenz Wiskott. Slowness and sparseness lead to place, head-direction, and spatial-view cells. *PLoS computational biology*, 3(8):e166, 2007.
- [5] Jonas Gehring, Michael Auli, David Grangier, Denis Yarats, and Yann N. Dauphin. Convolutional sequence to sequence learning. *CoRR*, abs/1705.03122, 2017.
- [6] Karol Gregor, Ivo Danihelka, Alex Graves, Danilo Jimenez Rezende, and Daan Wierstra. Draw: A recurrent neural network for image generation. *arXiv preprint arXiv:1502.04623*, 2015.
- [7] Karol Gregor, Ivo Danihelka, Alex Graves, Danilo Jimenez Rezende, and Daan Wierstra. Draw: A recurrent neural network for image generation. *arXiv preprint arXiv:1502.04623*, 2015.
- [8] Kaiming He, Xiangyu Zhang, Shaoqing Ren, and Jian Sun. Deep residual learning for image recognition. *CoRR*, abs/1512.03385, 2015.
- [9] Geoffrey E Hinton and Drew Van Camp. Keeping neural networks simple by minimizing the description length of the weights. In *Proceedings of the sixth annual conference on Computational learning theory*, pages 5–13. ACM, 1993.
- [10] Amy K Hoover and Kenneth O Stanley. Exploiting functional relationships in musical composition. *Connection Science*, 21(2-3):227–251, 2009.
- [11] Dan Horgan, John Quan, David Budden, Gabriel Barth-Maron, Matteo Hessel, Hado Van Hasselt, and David Silver. Distributed prioritized experience replay. *arXiv preprint arXiv:1803.00933*, 2018.
- [12] Max Jaderberg, Karen Simonyan, Andrew Zisserman, et al. Spatial transformer networks. In *Advances in neural information processing systems*, pages 2017–2025, 2015.
- [13] Justin Johnson, Bharath Hariharan, Laurens van der Maaten, Li Fei-Fei, C Lawrence Zitnick, and Ross Girshick. Clevr: A diagnostic dataset for compositional language and elementary visual reasoning. In *Computer Vision and Pattern Recognition (CVPR), 2017 IEEE Conference on*, pages 1988–1997. IEEE, 2017.
- [14] Tero Karras, Timo Aila, Samuli Laine, and Jaakko Lehtinen. Progressive growing of gans for improved quality, stability, and variation. In *ICLR*, volume abs/1710.10196, 2018.
- [15] Alex Krizhevsky, Ilya Sutskever, and Geoff Hinton. Imagenet classification with deep convolutional neural networks. In *Advances in Neural Information Processing Systems 25*, pages 1106–1114, 2012.
- [16] Yann LeCun, Yoshua Bengio, et al. Convolutional networks for images, speech, and time series. *The handbook of brain theory and neural networks*, 3361(10):1995, 1995.
- [17] Chunyuan Li, Heerad Farkhoor, Rosanne Liu, and Jason Yosinski. Measuring the Intrinsic Dimension of Objective Landscapes. In *International Conference on Learning Representations*, April 2018.
- [18] V. Mnih, K. Kavukcuoglu, D. Silver, A. Graves, I. Antonoglou, D. Wierstra, and M. Riedmiller. Playing Atari with Deep Reinforcement Learning. *ArXiv e-prints*, December 2013.

- [19] Volodymyr Mnih, Adria Puigdomenech Badia, Mehdi Mirza, Alex Graves, Timothy Lillicrap, Tim Harley, David Silver, and Koray Kavukcuoglu. Asynchronous methods for deep reinforcement learning. In *International Conference on Machine Learning*, pages 1928–1937, 2016.
- [20] A. Nguyen, J. Yosinski, Y. Bengio, A. Dosovitskiy, and J. Clune. Plug & Play Generative Networks: Conditional Iterative Generation of Images in Latent Space. *ArXiv e-prints*, November 2016.
- [21] Alec Radford, Luke Metz, and Soumith Chintala. Unsupervised representation learning with deep convolutional generative adversarial networks. *arXiv preprint arXiv:1511.06434*, 2015.
- [22] Scott E Reed, Zeynep Akata, Santosh Mohan, Samuel Tenka, Bernt Schiele, and Honglak Lee. Learning what and where to draw. In *Advances in Neural Information Processing Systems*, pages 217–225, 2016.
- [23] Shaoqing Ren, Kaiming He, Ross Girshick, and Jian Sun. Faster r-cnn: Towards real-time object detection with region proposal networks. In *Advances in neural information processing systems*, pages 91–99, 2015.
- [24] Jorma Rissanen. Modeling by shortest data description. *Automatica*, 14(5):465–471, 1978.
- [25] Adam Santoro, David Raposo, David G Barrett, Mateusz Malinowski, Razvan Pascanu, Peter Battaglia, and Tim Lillicrap. A simple neural network module for relational reasoning. In *Advances in neural information processing systems*, pages 4974–4983, 2017.
- [26] A. Sergeev and M. Del Balso. Horovod: fast and easy distributed deep learning in TensorFlow. *ArXiv e-prints*, February 2018.
- [27] Kenneth O Stanley. Compositional pattern producing networks: A novel abstraction of development. *Genetic programming and evolvable machines*, 8(2):131–162, 2007.
- [28] Aaron Van Den Oord, Sander Dieleman, Heiga Zen, Karen Simonyan, Oriol Vinyals, Alex Graves, Nal Kalchbrenner, Andrew Senior, and Koray Kavukcuoglu. Wavenet: A generative model for raw audio. *arXiv preprint arXiv:1609.03499*, 2016.
- [29] Ashish Vaswani, Noam Shazeer, Niki Parmar, Jakob Uszkoreit, Llion Jones, Aidan N Gomez, Łukasz Kaiser, and Illia Polosukhin. Attention is all you need. In *Advances in Neural Information Processing Systems*, pages 6000–6010, 2017.
- [30] Fisher Yu, Ari Seff, Yinda Zhang, Shuran Song, Thomas Funkhouser, and Jianxiong Xiao. Lsun: Construction of a large-scale image dataset using deep learning with humans in the loop. *arXiv preprint arXiv:1506.03365*, 2015.
- [31] Han Zhang, Tao Xu, Hongsheng Li, Shaoting Zhang, Xiaolei Huang, Xiaogang Wang, and Dimitris Metaxas. Stackgan: Text to photo-realistic image synthesis with stacked generative adversarial networks. In *IEEE Int. Conf. Comput. Vision (ICCV)*, pages 5907–5915, 2017.

# Supplementary Information for: An intriguing failing of convolutional neural networks and the CoordConv solution

## S1 Architectures used for supervised painting tasks

Figure S1 depicts different architectures used in each of the two supervised tasks going from coordinates to images. The same deconvolutional architecture for both tasks, but we generally found the Supervised Rendering tasks requires wider layers (more channels). Top performing deconvolutional models in Supervised Coordinate Classification have  $c = 1$  or  $2$ , while in Supervised Rendering we usually need  $c = 2, 3$ . In terms of convolutional filter size, filter sizes of  $2$  and  $4$  seem to outperform  $3$  in Coordinate Classification, while in Rendering the difference is less distinctive.

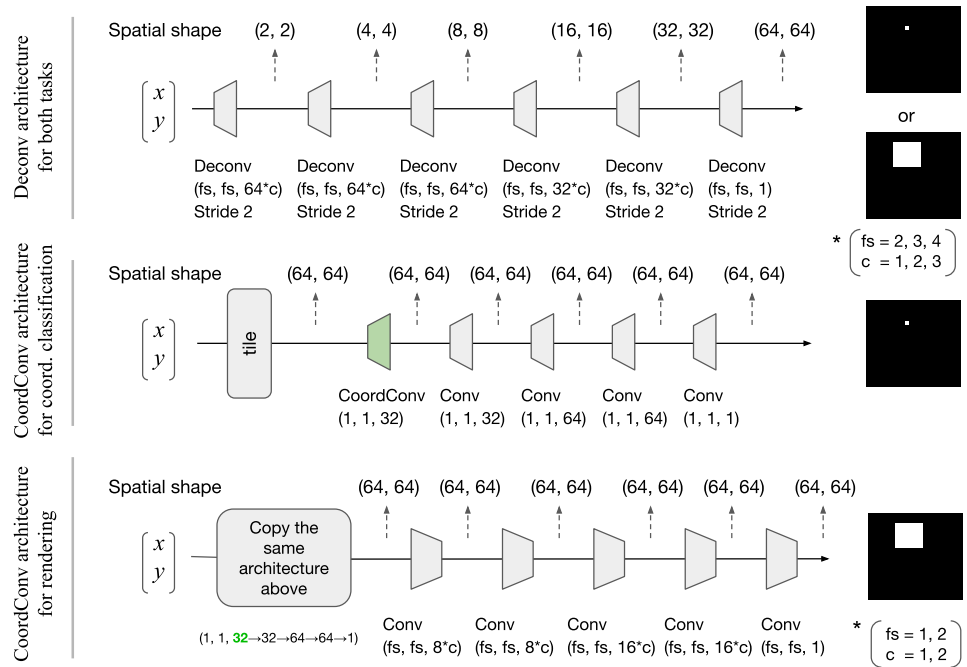


Figure S1: Deconvolutional and CoordConv architectures used in each of the two supervised tasks. “fs” stands for filter size, and “c” for channel size. We use a grid search on different ranges of them as displayed underneath each model, while allowing deconvolutional models a wider range in both. Green indicates a CoordConv layer.

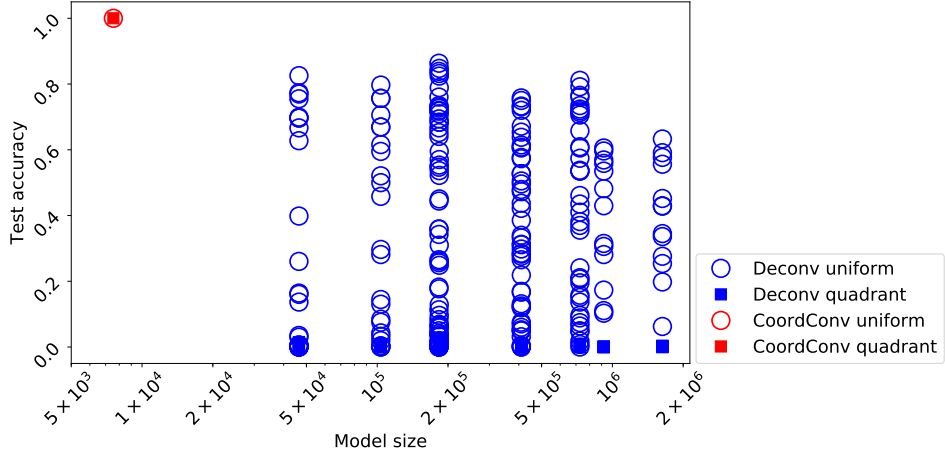


Figure S2: Model size vs. test accuracy for the Supervised Coordinate Classification subtask on the uniform split and quadrant split. Deconv models (blue) of many sizes achieve 80% or a little higher — but never perfect — test accuracy on the uniform split. On the quadrant split, while many models perform slightly better than chance ( $1/4096 = .000244$ ) no model generalizes significantly. CoordConv model achieves perfect accuracy on both splits.

Because of the usage of different filter sizes and channel sizes, we end up training models with a range of sizes. Each is combined with further grid searches on hyperparameters including the learning rate, weight decay, and minibatch sizes. Therefore at the same size we end up with multiple models with a spread of performances, as shown in Figure S2 for the Supervised Coordinate Classification task. We repeat the same exact setting of experiments on both uniform and quadrant splits, which result in the same number of experiments. It is not obviously shown in Figure S2 because quadrant trainings are mostly poorly (at the bottom of the figure).

As can be seen, it seems unlikely that even larger models would perform better. They all basically struggle to get to a good test accuracy. This (1) confirms that performance is not simply being limited by model size, as well as (2) shows that working CoordConv models are one to two orders of magnitude smaller (7553 as opposed to 50k-1.6M parameters) than the best convolutional models. The model size vs. test performance plot on Supervised Rendering is similar (not shown), except CoordConv model in that case has a slightly larger number of parameters: 9490. CoordConv achieves perfect test IOU there while deconvolutional models struggle at sizes 183k to 1.6M.

## S2 Further Supervised Coordinate Classification details

For deconvolutional models, we use the model structure as depicted in the top row in Figure S1, while varying the choice of filter size ( $\{2, 3, 4\}$ ) and channel size multipliers ( $\{1, 2, 3\}$ ), and each combined with a hyperparameter sweep of learning rate  $\{0.001, 0.002, 0.005, 0.01, 0.02, 0.05\}$ , and weight decay  $\{0.001, 0.01\}$ . Models are trained using a softmax output with cross entropy loss with Adam optimizer. We train 1000 epochs with minibatch size of 16 and 32. The learning rate is dropped to 10% every 200 epochs for four times.

For CoordConv models, because it converges so fast and easy, we did not have to try a lot of settings — only 3 learning rates  $\{0.01, 0.001, 0.005\}$  and they all learned perfectly well. There's also no need for learning rate schedules as it quickly converges in 10 seconds.

Figure S3 demonstrates how accurate and smooth the learned probability mass is with CoordConv, and not so much with Deconv. We first show the overall  $64 \times 64$  map of logits, one for a training example and one for a test example just right next to the train. Then we zoom in to a smaller region to examine the intricacies. We can see that convolution, even though designed to act in a translation-invariant way, shows artifacts of not being able to accomplish so.

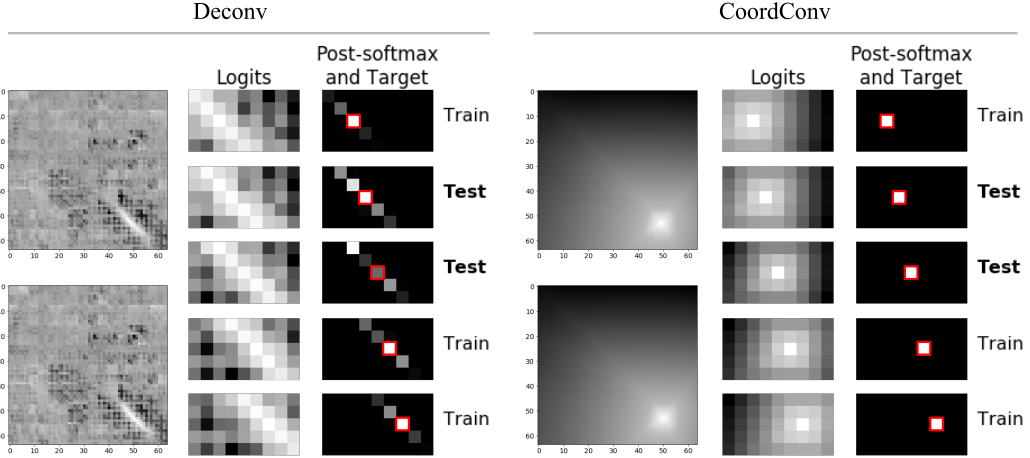


Figure S3: Comparison of behaviors between Deconv model and CoordConv model on the Supervised Coordinate Classification task. We select five horizontally neighboring pixels, containing samples in both train and test splits, and zoom in on a  $5 \times 9$  section of the  $64 \times 64$  canvas so the detail of the logits and predicted probabilities may be seen. The full  $64 \times 64$  map of logits of the first two samples (first in train, second in test) are also shown. The deconvolutional model outputs probabilities in a decidedly non-translation-invariant manner.

### S3 Further Supervised Coordinate Regression details

Exact architectures applied in the Supervised Coordinate Regression task are described in table S1. For the uniform split, the best-generalizing convolution architecture consisted of a stack of alternating convolution and max-pooling layers, followed by a fully-connected layer and an output layer. This architecture was fairly robust to changes in hyperparameters. In contrast, for the quadrant split, the best-generalizing network consisted of strided convolutions feeding into a global-pooling output layer, and good performance was delicate. In particular, training and generalization was sensitive to the number of batch normalization layers (2), weight decay strength (5e-4), and optimizer (Adam, learning rate 5e-4). A single CoordConv architecture generalized perfectly with the same hyperparameters over both splits, and consisted of a signle CoordConv layer followed by additional layers of convolution, feeding into a global pooling output layer.

Table S1: Model Architectures for Supervised Coordinate Regression. FC: Fully-connected, MP: Max Pooling, GP: Global Pooling, BN: Batch normalization, s2: stride 2.

	Conv	CoordConv
Uniform Split	$3 \times 3, 16 - \text{MP } 2 \times 2 - 3 \times 3, 16 - \text{MP } 2 \times 2 - 3 \times 3,$ $16 - \text{MP } 2 \times 2 - 3 \times 3, 16 - \text{FC } 64 - \text{FC } 2$	$1 \times 1, 8 - 1 \times 1, 8 - 1 \times 1, 8 - 3 \times 3,$ $8 - 3 \times 3, 2 - \text{GP}$
Quadrant Split	$5 \times 5 (\text{s2}), 16 - 1 \times 1, 16 - \text{BN} - 3 \times 3, 16 - 3 \times 3$ (s2), $16 - 3 \times 3 (\text{s2}), 16 - \text{BN} - 3 \times 3 (\text{s2}), 16 -$ $1 \times 1, 16 - 3 \times 3 (\text{s2}), 16 - 3 \times 3, 2 - \text{GP}$	

### S4 Further Supervised Rendering details

The experimental setting is similar to Section S2 except the loss used is pixelwise sigmoid output with cross entropy loss. We also tried mean squared error loss but the performance is even weaker. We performed heavy hyperparameter sweeping and deliberate learning rate annealing for Deconv models (same as said in Section S2), while in CoordConv models it is fairly easy to find a good setting. All models trained with learning rates {0.001, 0.005}, weight decay {0, 0.001}, filter size {1, 2} turned out to perform well after 1–2 minutes of training. Figure S4 and Figure S5 show the learned logits

and pixelwise probability distributions for three samples each, in the uniform and quadrant cases, respectively. We can see that the CoordConv model learns a much smoother and precise distribution. All samples are test samples.

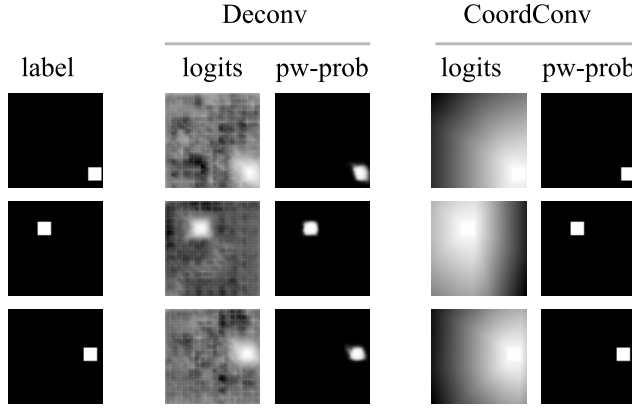


Figure S4: Output comparison between Deconv and CoordConv models on three test samples. Models are trained on a *uniform* split. Logits are model’s direct output; pixelwise probability (pw-prob) is logits after Sigmoid. Conv outputs (middle columns) manage to get roughly right. CoordConv outputs (right columns) are precisely correct and its logit maps are smooth.

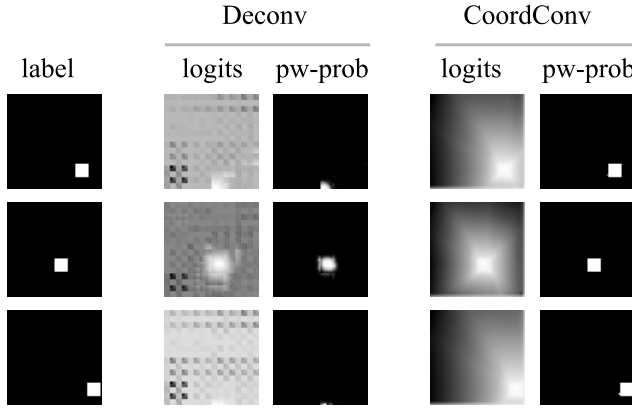


Figure S5: Output comparison between Deconv and CoordConv models on three test samples. Models are trained on a *quadrant* split. Logits are model’s direct output; pixelwise probability (pw-prob) is logits after Sigmoid. Conv outputs (middle columns) failed mostly. Even with such a difficult generalization problem, CoordConv outputs (right columns) are precisely correct and its logit maps are smooth.

## S5 Further ImageNet classification details

We evaluate the potential of CoordConv in image classification with ImageNet experiments. We take ResNet-50 and run the baseline on distributed framework using 100 GPUs, with the open-source framework Horovod. For CoordConv variants, we add an extra CoordConv layer only in the beginning, which takes a 6-channel tensor containing image RGB,  $i, j$  coordinates and pixel distance to center  $r$ , and output 8 channels with  $1 \times 1$  convolution. The increase of parameters is negligible. It then goes in with the rest of ResNet-50.

Each model is run 5 times on the same setting to account for experimental variances. Table. S2 lists the test result from each run in the end of 90 epochs. CoordConv model obtains better average result on two of the three measures, however a one-sided t-test tells that the improvement on Top 5 accuracy is not quite statistically significant with  $p = .11$ . Here we didn’t expect

Of all vision tasks, we might expect image classification to show the least performance change when using CoordConv instead of convolution, as classification is more about what is in the image than where it is. This tiny amount of improvement validates that.

Table S2: ImageNet classification result comparison between a baseline ResNet-50 and CoordConv ResNet-50. For each model three experiments are run, listed in three separate rows below.

	Test loss	Top-1 Accuracy	Top-5 Accuracy
Baseline ResNet-50	1.43005	0.75722	0.92622
	1.42385	0.75844	0.9272
	1.42634	0.75782	0.92754
	1.42166	0.75692	0.92756
	1.42671	0.75724	0.92708
Average	1.425722	<b>0.757528</b>	0.92712
CoordConv ResNet-50	1.42335	0.75732	0.92802
	1.42492	0.75836	0.92754
	1.42478	0.75774	0.92818
	1.42882	0.75702	0.92694
	1.42438	0.75668	0.92714
Average	<b>1.42525</b>	0.757424	<b>0.927564</b>

## S6 Further object detection details

The object detection experiments are on a dataset containing randomly rescaled and placed MNIST digits on a  $64 \times 64$  canvas. To make it more akin to natural images, we generate a much larger canvas and then center crop it to be  $64 \times 64$ , so that digits can be partially outside of the canvas. We kept images that contain 5 digit objects whose centers are within the canvas. In the end we use 9000 images as the training set and 1000 as test.

A schematic of the model architecture is illustrated in Figure S6. We use number of anchors  $A = 9$ , with sizes  $(15, 15)$ ,  $(20, 20)$ ,  $(25, 25)$ ,  $(15, 20)$ ,  $(20, 25)$ ,  $(20, 15)$ ,  $(25, 20)$ ,  $(15, 25)$ ,  $(25, 15)$ . In box sampling (training mode),  $p\_size$  and  $n\_size$  are 6. In box non-maximum suppression (NMS) (test mode), the IOU threshold is 0.8 and maximum number of proposal boxes is 10. After the boxes are proposed and shifted, we do not have a downstream classification task, but just calculate the loss from the boxes. The training loss include box loss and score loss. As evaluation metric we also calculate IOUs between proposed boxes and ground truth boxes. Table. S3 lists those metrics obtained the test dataset, by both Conv and CoordConv models. We found that every metric is improved by CoordConv, and the average test IOU improved by about 24 percent.

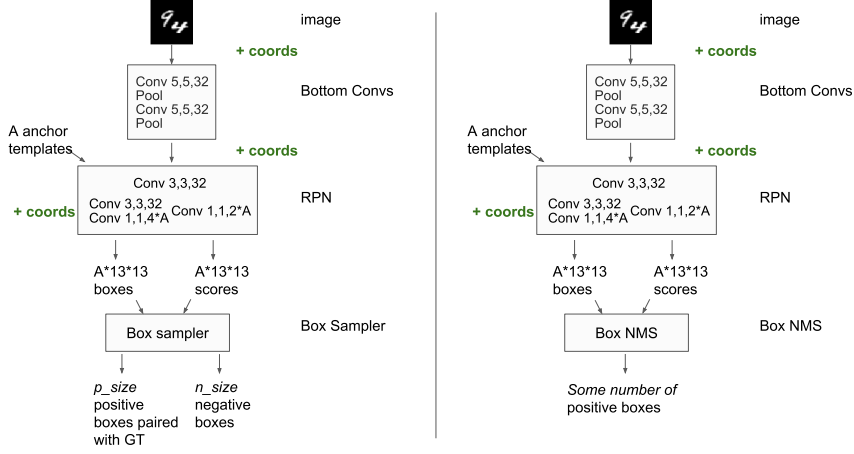


Figure S6: Faster R-CNN architecture used for object detection on scattered MNIST digits. Green indicates where coordinates are added. (**Left**) train mode with box sampler. (**Right**) test mode with box NMS.

Table S3: MNIST digits detection result comparison between a Faster R-CNN model with regular convolution vs. with CoordConv. Metrics are all on test set. Train IOU: average IOU between sampled positive boxes (train mode) and ground truth; Test IOU-average): average IOU between 10 selected boxes (test mode) and ground truth; Test IOU-select: average IOU between the best scored box and its closest ground truth.

	Conv	CoordConv	% Improvement
Box loss	0.1003	0.0854	17.44
Score loss	0.5270	0.2526	108.63
Total loss (sum of the two above)	0.6271	0.3383	85.37
Train IOU	0.6388	0.6612	3.38
Test IOU-average	0.1508	0.1868	23.87
Test IOU-select	0.4965	0.6359	28.08

## S7 Further generative modeling details

### S7.1 GANs on colored shapes

The dataset used to train the generative models is 50k red-and-blue-object images of size  $64 \times 64$ . We follow the same mechanism as Sort-of-Clevr, in that objects appear at random positions on a white background without overlapping, only limiting the number of objects to be 2 per image. The objects are always one red and one blue, of a randomly chosen shape out of {circle, square}. Examples of images from this dataset can be seen in the top row, leftmost column in Figure 7, at the intersection of “Real images” and “Random samples”.

The  $z$  dimension to both regular GAN and CoordConv GAN is 256. In GAN, the generator uses 4 layers of deconvolution with strides of 2 to project  $z$  to a  $64 \times 64$  image shape. The parameter size of the generator is 6,413,315. In CoordConv GAN, we add coordinate channels only at the beginning, making the first layer CoordConv, and then continue with normal Conv.. The generator in this case uses mostly (1,1) convolutions and has only 444,931 parameters. The same discriminator is used for both models. In the case where we also turn the discriminator to be CoordConv like, its first Conv layer is replaced by CoordConv, and the parameter size increases from 4,316,545 to 4,319,745. The details of both architectures can be seen in Table. S4. We trained two CoordConv GAN versions

where CoordConv applies: 1) only in generator, and 2) in both generator and discriminator. They end up performing similarly well. The demonstrated examples in all figures are from one in the latter case.

The change needed to make a generator whose first layer is fully-connected CoordConv is trivial. Instead of taking image tensors which already have Cartesian dimensions, the CoordConv generator first tiles  $z$  vector into a full  $64 \times 64$  space, and then concatenate it with coordinates in that space.

To train each model we use a fixed learning rate 0.0001 for the discriminator and 0.0005 for the generator. In each iteration discriminator is trained once followed by generator trained twice. The random noise vector  $z$  is drawn from a uniform distribution between  $[-1, 1]$ . We train each model for 50 epochs and save the model in the end of every epoch. We repeat the training with the same hyperparameters 5 to 10 times for each, and pick the best model for each to show a fair comparison in all figures.

Table S4: Model Architectures for GAN and CoordConv GAN used in the colored shape generation. In the case of CoordConv GAN, only the first layer is changed from regular Conv to CoordConv. FC: fully connected layer; s2: stride 2.

	Generator	Discriminator
GAN	FC 8192 (reshape $4 \times 4 \times 512$ ) - $5 \times 5$ , 256 (s2) - $5 \times 5$ , 128 (s2) - $5 \times 5$ , 64 (s2) - $5 \times 5$ , 3 (s2) - Tanh	$5 \times 5$ , 64 (s2) - $5 \times 5$ , 128 (s2) - $5 \times 5$ , 256 (s2) - $5 \times 5$ , 512 (s2) - 1
CoordConv GAN	$1 \times 1$ , 512 - $1 \times 1$ , 256 - $1 \times 1$ , 256 - $1 \times 1$ , 128 - $1 \times 1$ , 64 - $3 \times 3$ , 64 - $3 \times 3$ , 64 - $1 \times 1$ , 3	

The latent interpolation is conducted by randomly choosing two noise vectors, each from a uniform distribution, and linearly interpolate in between with an  $\alpha$  factor that indicates how close it is to the first vector. Figure S7, Figure S8 each show five random samples of pairs to conduct interpolation with. And Figure S8 shows deliberately picked examples that exhibit a special moving effect that has only been seen in CoordConv GAN.

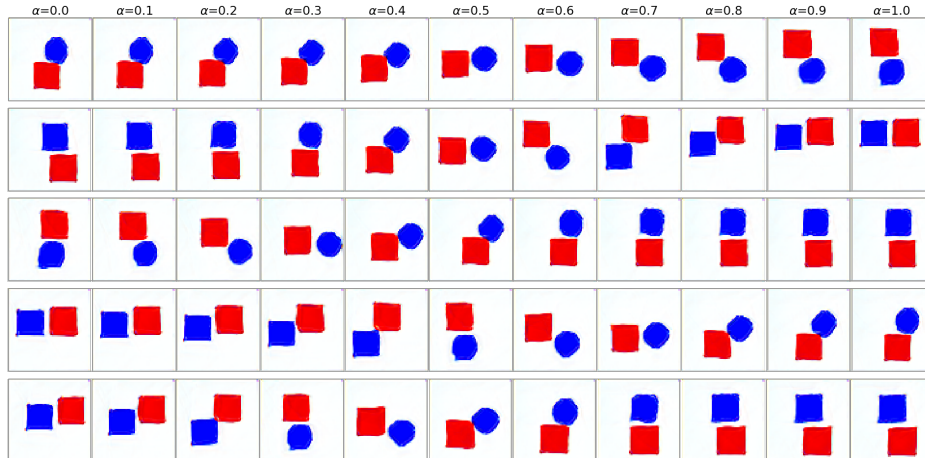


Figure S7: CoordConv GAN samples with a series of interpolation between 5 random pairs of  $z$ . Top row: at the position in the manifold, the model has learned a smooth circular motion. The rest of the rows: the circular relation between two objects is still observed, while some object shapes also undergo a smooth transition.

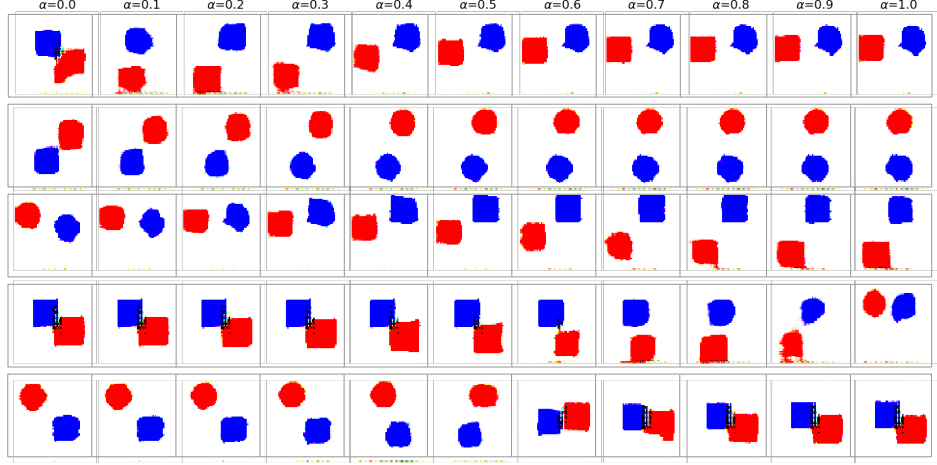


Figure S8: Regular GAN samples with a series of interpolation between 5 random pairs of  $z$ . Also observed position and shape transitioning but are different.

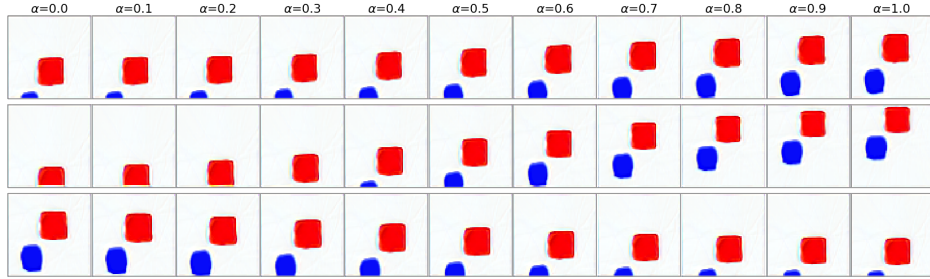


Figure S9: A special effect only observed in CoordConv GAN latent space interpolation: two objects stay constant in relative positions to each other but move together in space. They even move out of the scene which is never present in the real data — learned to extrapolate. These 3 examples are picked from many random drawings of  $z$  pairs, as opposed to Figure S7 and Figure S8, where first 5 random drawings are shown.

## S7.2 VAEs on colored shapes

Convolutional VAEs trained on the same dataset as above in Section S7.1 exhibit many of the same problems that we observed in GANs, and adding CoordConv confers many of the same benefits.

A VAE is composed of an encoder that maps data to a latent and a decoder that maps the latent back to data. With minor exceptions our VAE’s encoder architecture is the same as our GAN’s discriminator and it’s decoder is the same as our GAN’s generator. The important difference is of course that the output shape of the encoder is the size of the latent (in this case 8), not two as in a discriminator.

The decoder architectures of the convolutional control and coordconv experiments are similar aside from kernel size - the CoordConv decoder uses 1x1 kernels while the convolutional decoder uses 5x5 kernels.

As described in S.6, the VAE was trained on 50k 64 x 64 images of blue and red non-overlapping squares and circles.

Due to the pixel sparsity of images in the dataset we found it important to weight reconstruction loss more heavily than latent loss by a factor of 50. Doing so didn’t interfere with the quality of the encoding. We used Adam with a learning rate of 0.005 and no weight decay.

Table S5: Model Architectures: Convolutional VAE and CoordConv VAE

	Decoder	Encoder
VAE	FC 8192 (reshape $4 \times 4 \times 512$ ) - $5 \times 5$ , 256 (s2) - $5 \times 5$ , 128 (s2) - $5 \times 5$ , 64 (s2) - $5 \times 5$ , 3 (s2) - Sigmoid	$5 \times 5$ , 64 (s2) - $5 \times 5$ , 128 (s2) - $5 \times 5$ , 256 (s2) - $5 \times 5$ , 512 (s2) - Flatten - FC, 10
CoordConv VAE	$1 \times 1$ , 512 - $1 \times 1$ , 256 - $1 \times 1$ , 256 - $1 \times 1$ , 128 - $1 \times 1$ , 64 - $1 \times 1$ , 3 - Sigmoid	

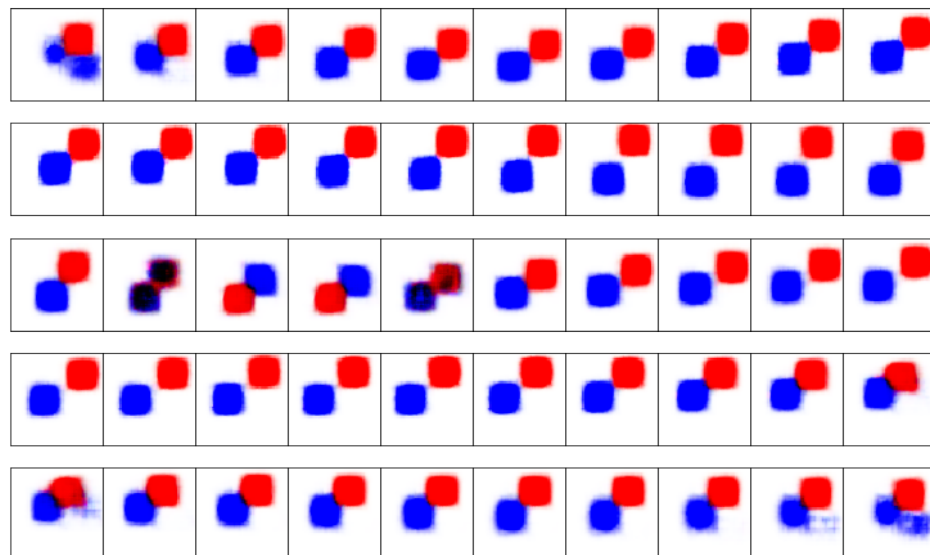


Figure S10: Latent space interpolations from a VAE without CoordConv. The red and blue shapes are mostly stationary. When they do move they do so by disappearing and appearing elsewhere in pixel space. Smooth changes in the latent don't translate to smooth geometric changes in pixel space. The latents we interpolated between were sampled randomly from a uniform distribution.

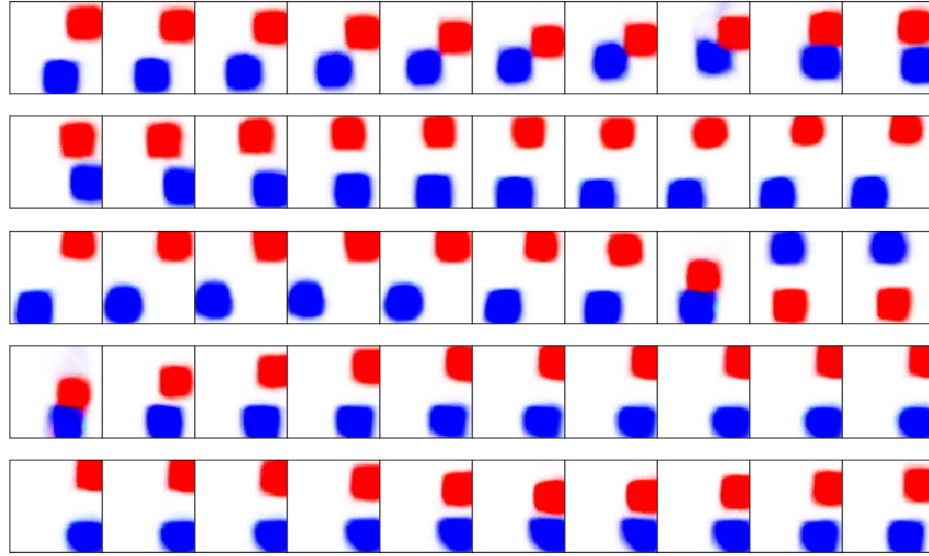


Figure S11: Latent space interpolations from a VAE with CoordConv in the encoder and decoder. The red and blue shapes span pixel space more fully and smooth changes in latent space map to smooth changes in pixel space. Like the CoordConv GAN, the CoordConv VAE is able to extrapolate beyond the borders of the frame it was trained on. The latents we interpolated between were sampled randomly from a uniform distribution.

### S7.3 GANs on LSUN

The dataset used to train the generative models is LSUN bedroom, composed of 3,033,042 images of size  $64 \times 64$ .

The architectures adopted are really similar to the ones adopted for generating the colored shape results in Section S7.1, with few noticeable differences:

- we use CoordConv layers instead of regular Conv layers not only in the first layer of the discriminator, but in each layer.  $z$  is of dimension 100.
- the GAN generator includes a layer mapping from  $z$  to a  $4 \times 4 \times 1024$  tensor and the other layers have double the number of channels.
- CoordConv GAN generator has more channels for each layer.

Table S6: Model Architectures for GAN and CoordConv GAN for LSUN. FC: fully connected layer; s2: stride 2.

	Generator	Discriminator
GAN	FC 16384 (reshape $4 \times 4 \times 1024$ ) - $5 \times 5$ , 512 (s2) - $5 \times 5$ , 256 (s2) - $5 \times 5$ , 128 (s2) - $5 \times 5$ , 3 (s2) - Tanh	$5 \times 5$ , 64 (s2) - $5 \times 5$ , 128 (s2) - $5 \times 5$ , 256 (s2) - $5 \times 5$ , 512 (s2) - 1
CoordConv GAN	$1 \times 1$ , 1024 - $1 \times 1$ , 512 - $1 \times 1$ , 256 - $1 \times 1$ , 256 - $1 \times 1$ , 128 - $3 \times 3$ , 128 - $3 \times 3$ , 64 - $1 \times 1$ , 3	



Figure S12: Samples from the regular GAN (left) and the CoordConv GAN (right).

Samples from both models are provided in Figure S12. One peculiar property of the CoordConv GAN model with respect to the regular GAN one is the geometric interpolation. As shown in Figure Figure S13 in regular GAN interpolations objects appear and disappear, while in CoordConv GAN interpolations in Figure S14 objects move around, translating, enlarging, squashing and doing geometric transformations over them.

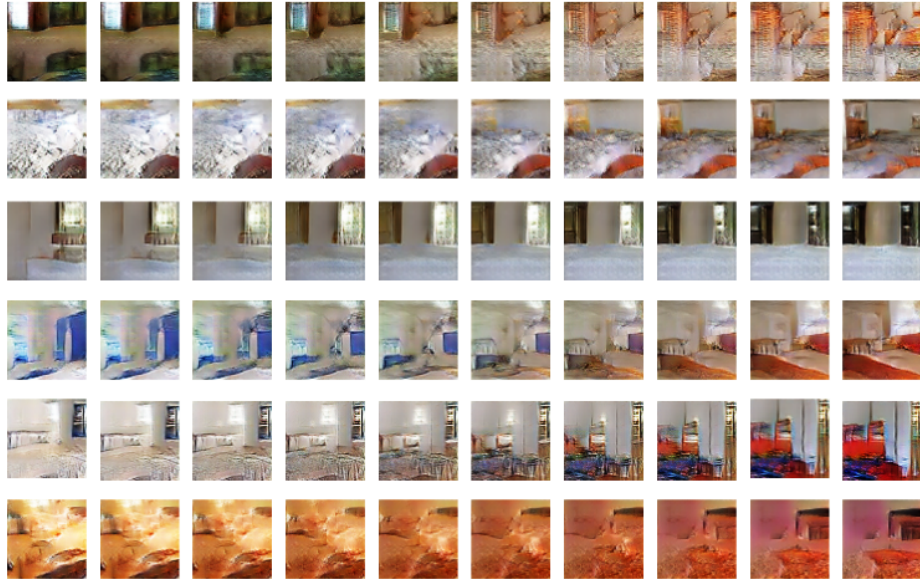


Figure S13: Samples of regular GAN trained on LSUN with a series of interpolation between 5 random pairs of  $z$ .

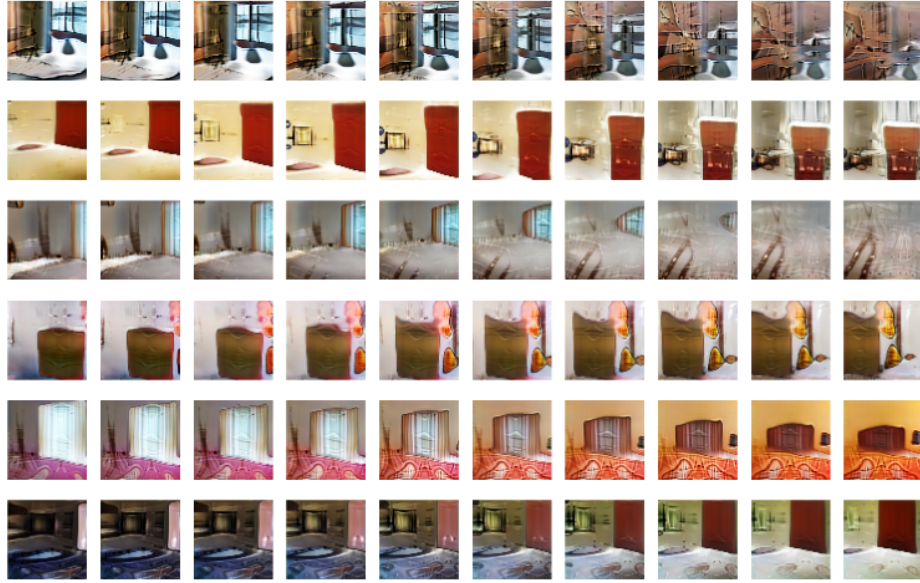


Figure S14: Samples of CoordConv GAN trained on LSUN with a series of interpolation between 5 random pairs of  $z$ .

The regular GAN has been trained for 11000 steps of batch size 128, while the CoordConv GAN has been trained 22000 steps of batch size 64 (because the available memory on the GPUs did not allow for 128). Both models have been trained using Horovod to distribute the training on 16 GPUs.

## S8 The CoordConv layer implementation

```

from tensorflow.python.layers import base
import tensorflow as tf

class AddCoords(base.Layer):
    """Add coords to a tensor"""
    def __init__(self, x_dim=64, y_dim=64, with_r=False):
        super(AddCoords, self).__init__()
        self.x_dim = x_dim
        self.y_dim = y_dim
        self.with_r = with_r

    def call(self, input_tensor):
        """
        input_tensor: (batch, x_dim, y_dim, c)
        """
        batch_size_tensor = tf.shape(input_tensor)[0]
        xx_ones = tf.ones([batch_size_tensor, self.x_dim],
                          dtype=tf.int32)
        xx_ones = tf.expand_dims(xx_ones, -1)
        xx_range = tf.tile(tf.expand_dims(tf.range(self.x_dim), 0),
                           [batch_size_tensor, 1])
        xx_range = tf.expand_dims(xx_range, 1)

        xx_channel = tf.matmul(xx_ones, xx_range)
        xx_channel = tf.expand_dims(xx_channel, -1)

```

```

yy_ones = tf.ones([batch_size_tensor, self.y_dim],
                  dtype=tf.int32)
yy_ones = tf.expand_dims(yy_ones, 1)
yy_range = tf.tile(tf.expand_dims(tf.range(self.y_dim), 0),
                   [batch_size_tensor, 1])
yy_range = tf.expand_dims(yy_range, -1)

yy_channel = tf.matmul(yy_range, yy_ones)
yy_channel = tf.expand_dims(yy_channel, -1)

xx_channel = tf.cast(xx_channel, 'float32') / (self.x_dim - 1)
yy_channel = tf.cast(yy_channel, 'float32') / (self.y_dim - 1)
xx_channel = xx_channel*2 - 1
yy_channel = yy_channel*2 - 1

ret = tf.concat([input_tensor,
                 xx_channel,
                 yy_channel], axis=-1)

if self.with_r:
    rr = tf.sqrt( tf.square(xx_channel-0.5)
                  + tf.square(yy_channel-0.5)
                  )
    ret = tf.concat([ret, rr], axis=-1)

return ret

class CoordConv(base.Layer):
    """CoordConv layer as in the paper."""
    def __init__(self, x_dim, y_dim, with_r, *args, **kwargs):
        super(CoordConv, self).__init__()
        self.addcoords = AddCoords(x_dim=x_dim,
                                  y_dim=y_dim,
                                  with_r=with_r)
        self.conv = tf.layers.Conv2D(*args, **kwargs)

    def call(self, input_tensor):
        ret = self.addcoords(input_tensor)
        ret = self.conv(ret)
        return ret

```